WIRELESS COMMUNICATIONS AND MOBILE COMPUTING
Wirel. Commun. Mob. Comput. 2011; **11**:1540–1550
Published online 15 November 2011 in Wiley Online Library (wileyonlinelibrary.com). DOI: 10.1002/wcm.1215

SPECIAL ISSUE PAPER

Mobile free space optic nodes in single-input multiple-output setup under transmitter misalignment

Hassan Moradi[1]*, Hazem H. Refai[1], Peter G. LoPresti[2] and Mohammed Atiquzzaman[3]

[1] Electrical and Computer Engineering, University of Oklahoma, Tulsa, OK, U.S.A.
[2] Electrical Engineering Department, University of Tulsa, Tulsa, OK, U.S.A.
[3] Computer Science, University of Oklahoma, Norman, OK, U.S.A.

ABSTRACT

Wireless optical nodes with mobility capabilities (mobile free space optics [FSO]) have emerged as a way to overcome limitations inherent in FSO links, for example, transmitter–receiver restrictive alignment requirement. This paper proposes the use of an angular diversity model for characterizing the performance of mobile FSO over atmospheric turbulence, and transmitter–receiver misalignment switch-and-examine combining technique is suggested for a diversity combining under unbalanced multireceiving configuration. A laser beam is modeled as spatial Gaussian profile, and channel fading is modeled as a lognormal distribution with spatially uncorrelated samples. Analytical and statistical discussion on the resultant output is presented, and bit error performance and processing load are numerically evaluated and compared with those obtained using selection combining diversity schemes. Copyright © 2011 John Wiley & Sons, Ltd.

KEYWORDS

mobile FSO; misalignment; channel state information (CSI); switched diversity; switch-and-examine combining (SEC); selection combining (SC)

***Correspondence**

Hassan Moradi, Electrical and Computer Engineering, University of Oklahoma, Tulsa, OK, U.S.A.
E-mail: hmoradi@ou.edu

1. INTRODUCTION

Wireless optical communication, that is, free space optics (FSO), offers significant advantages over radio frequency (RF) communication, including unlicensed frequency spectrum and high data rate transmission. However, line-of-sight connection and the directional reception of narrow FSO beams are major deterrents to the practical development of mobile communication. Classified as single input multiple output (SIMO), mobile FSO offers mobility to an optical network. Asymmetrically unbalanced receiver apertures with intentional misalignment are installed to establish node mobility while maintaining optical connection.

Free space optic-based mobile nodes can potentially be used in a mobile ad hoc network where an infrastructure is unavailable [1] and/or in a wireless sensor network where communication security, including freedom from susceptibility to jamming, is important [2]. Previous works on mobile FSO focus mainly on alignment and tracking issues [3] and on the design of multielement structure [4,5], which are characterized to ensure uninterrupted data flow by auto-aligning transmitter and receiver modules. These solutions concentrate on design and/or experimental setups based on a simple deterministic angular diversity model. The unbalanced multireceiving structure of optical power distribution in a nonrandom model is characterized in [6]. The work presented in this paper introduces random atmospheric turbulence into the unbalanced diversity model of mobile FSO, where branches have unequal attenuation coefficients.

Because mobile FSO can be modeled as multireceiving spatial diversity, an efficient diversity-combining scheme is required to improve performance. When compared with all diversity techniques, maximum ratio combining—also known as optimal combining—provides superior combining performance. However, implementation complexities are inherent, and the system is extremely sensitive to channel estimation error. This is especially true for low signal-to-noise ratio (SNR) signals. Equal gain combining could be considered as a proposed candidate for FSO where the output SNR of the combiner is averaged over all receiving branches. As a result, it is plausible that a certain number of very low SNRs—due to misalignment—can cause a severe

drop in output SNR. Equal gain combining is, therefore, inefficient for systems with branches having acutely low SNR values. Selection combining (SC), as the name suggests, adheres to a selection strategy wherein the scheme continuously switches to the branch with the highest SNR. Even though the SC process is seemingly simple, the high processing load and repetitive switching characterized in SC diversity may not support the high data transmission rates achievable in FSO communication.

This paper investigates the feasibility study of deploying a switch-and-examine combining (SEC) diversity technique for mobile FSO. When an SEC scheme is employed, branch switching is initiated only when the active branch SNR drops below a defined threshold, thus limiting the switching repetitiveness that persists in an SC scheme. An SEC receiver examines in sequence the SNR of each of its branches and switches to the branch with an SNR deemed acceptable.

We assume a circular configuration of receiver apertures placed on the same plane. Intensity modulation is used for transmitting user binary information through a free space. It should be noted that because modulation format is independent of intensity modulation/direct detection scheme, it is outside the scope of this paper.

The balance of this paper is organized as follows. Section 2 offers channel model consideration. Section 3 presents misalignment statistics for transmitter and receiver relative to probability distribution. A combining approach for diversity in mobile FSO can be found in Section 4. Section 5 presents the simulation results, and Section 6 concludes the paper.

2. SYSTEM MODEL

The proposed mobile FSO node is constructed using unbalanced receiver apertures installed to provide angular diversity and is assumed to maintain connectivity under limited mobility over atmospheric turbulence conditions. This section offers a brief review of the node structure and channel model as they relate to mobile FSO.

2.1. Node structure

Various configurations can be considered for mobile FSO in an ad hoc network. We assume that mobile FSO have a circular layout and that receiving apertures are placed on a plane with the transmitter. The transmitter is a single branch node transmitting a Gaussian beam. The resultant setup denotes a SIMO configuration. Any two adjacent receiver apertures are separated by angles $\{\theta\}_{n=1}^{N}$ on a framework, as shown in Figure 1.

The electrical signal of the nth receiver expressed in discrete time samples is

$$r_n = 2RP_t h_n \alpha_n \beta_n s + v_n, \quad n = 1, 2, \ldots, N \qquad (1)$$

where $h_n > 0$ is the normalized time-varying channel fading coefficient associated with the nth receiver; v_n is the total additive Gaussian noise (mean I_0 and variance σ_v^2) associated with the nth receiver; α_n is the misalignment coefficient resulting from angular reception; β_n is the attenuation coefficient due to transmitter misalignment; R is the receiver's responsivity; and P_t is the average optical power equal for each branch. For simplicity, we include $2RP_t = 1$ to normalize the power. Note that the notation of the discrete-time index is neglected in model (1).

2.2. Channel model

The transmitter–receiver optical channel affected by atmospheric turbulence is given by $h = e^{2\chi}$, where log-amplitude χ is a normal random variable (RV) with mean μ_χ and standard deviation σ_χ, that is, "fading strength" or "Rytov variance/parameter" in the literature. The selection of $E[h] = 1$ leads us to $\mu_\chi = -\sigma_\chi^2$. Instantaneous

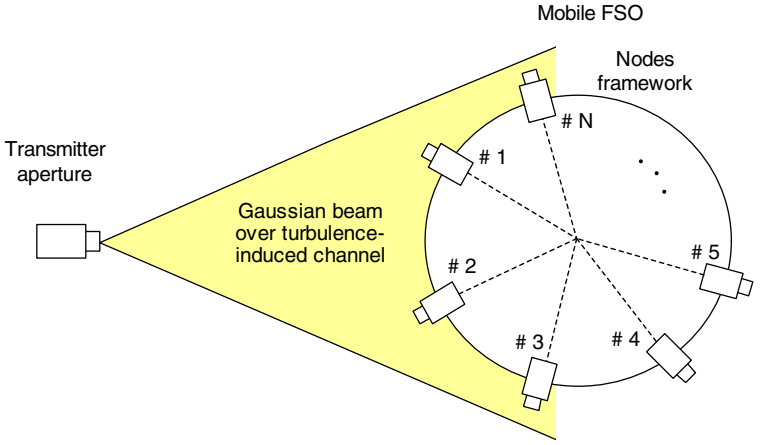

Figure 1. Illustration of mobile free space optics (FSO) in a single-input multiple-output setup.

electrical SNR will be defined by

$$\gamma_n = \bar{\gamma}\beta_n^2\alpha_n^2 h_n^2 \tag{2}$$

where, in our analysis, $\bar{\gamma}$ is defined as the average branch SNR, excluding fading effect and misalignment attenuation

$$\bar{\gamma} \triangleq \frac{R^2 P_t^2}{\sigma_v^2} \tag{3}$$

while using on–off keying modulation. For such a configuration, channel state information (CSI) is defined as

$$\{\gamma_n\}_{n=1}^N \tag{4}$$

Knowledge of CSI equivalently leads to finding $\{\alpha_n\beta_n h_n\}_{n=1}^N$.

We assume all N paths are independent and identically distributed. Lognormal distribution is considered to represent average atmospheric turbulence statistics, that is, scintillation for the channel coefficient, with a probability distribution function (PDF) in the form of [7]

$$f_{h_n}(h_n) = \frac{1}{\sqrt{8\pi}h_n\sigma_\chi}\exp\left[-\frac{\left(\ln(h_n)+2\sigma_\chi^2\right)^2}{8\sigma_\chi^2}\right] \tag{5}$$

The expression for the PDF of h_n^2 can easily be found, where $h_n^2 = e^{4\chi_n}$, deduced from Equation (5) by

$$f_{h_n^2}(h_n) = \frac{1}{\sqrt{32\pi}h_n^2\sigma_\chi}\exp\left[-\frac{\left(\ln(h_n)+2\sigma_\chi^2\right)^2}{8\sigma_\chi^2}\right] \tag{6}$$

Channel coefficients are essentially correlated in time and space domains as a result of atmospheric eddy movement. Temporal correlativeness may affect optimal detection performance when a single-input single-output system is investigated [7]. Spatial correlativeness should be considered when a spatial-based diversity system is used to demonstrate improved detection performance. Two important parameters—correlation (coherence) time and correlation length—in particular, represent the variation of the time-varying fading channel in time and space domain, respectively. These are related on the basis of Taylor's hypothesis by $\tau_0 = d_0/u_\perp$ [8], where τ_0 is correlation time; d_0 is correlation length; and $u_\perp$ is the perpendicular component of the wind velocity vector to the propagation direction.

The mutual covariance function between the log-amplitudes χ_i and χ_j of any two fading coefficients h_i and h_j associated with any two branches i and j is defined by $C_{i,j} \triangleq E[\chi_i\chi_j] - E[\chi_i]E[\chi_j]$. Note that $C_{i,j} = C_{j,i}$, because of the symmetry property of correlation. The correlation coefficient is defined as $\rho_{i,j} \triangleq C_{i,j}/\sigma_x^2, 0 \le \rho_{i,j} \le 1$. Given correlation length d_0, the correlation coefficient can be expressed under some conditions by $\rho = e^{-(d/d_0)^{5/3}}$ [9]. Correlation length d_0 becomes the distance at which the channel correlation coefficient is equal to e^{-1} and is approximated by the Fresnel length $d_0 \approx \sqrt{\lambda L}$. For instance, with a propagation path length, L, of 1 km and an optical wavelength of 830 nm, the fading correlation length is approximated by $d_0 = 2.4$ cm, that is, the receiver spacing required for uncorrelated scintillation should be farther than 2.89 cm.

3. MISALIGNMENT STATISTICS

For the bit error rate (BER) performance of the mobile FSO over a communication link to be evaluated, the branch SNR PDF is required. In turn, the branch SNR, γ_n, in Equation (2) is dependent upon the PDF of h_n^2, a_n^2, and β_n^2. These variables can be confidently assumed uncorrelated. In this case, with the aid of [10, Example 7], such an SNR for a given receiving branch n has a PDF in terms of a two-dimensional integral form of

$$f_{\gamma_n}(\gamma_n) = \frac{1}{\bar{\gamma}}\int_0^1 \frac{1}{\beta_2^n} f_{\beta_2^n}\left(\frac{\gamma_n}{\beta_n^2}\right)\int_0^1 \frac{1}{\alpha_n^2} f_{h^2}(\alpha_n) f_{\alpha_n^2} \times \left(\frac{\beta_n^2}{\bar{\gamma}\alpha_n^2}\right) \mathrm{d}\alpha_n \mathrm{d}\beta_n \tag{7}$$

The following section centers on the statistical analysis of misalignment characterization resulting from FSO mobility, as well as beam misalignment imposed by the transmitter. As such, overall branch SNR statistics can ultimately be characterized.

3.1. Mobile free space optic misalignment

Mobile FSO angular diversity design implies that receiving branches are not perfectly aligned to the transmitter. In Equation (1), $\alpha_n, 0 \le \alpha_n \le 1$, was defined as the attenuation factor of the nth receiver because of either misalignment or angular reception. Specifically, the misalignment coefficient α_n for any receiver aperture n directly relates to its azimuth angle in the transmission plane [2],

$$\alpha_n = \begin{cases} \exp(-\varphi_n^2), & -\frac{\pi}{2} < \varphi_n < \frac{\pi}{2} \\ 0, & \frac{\pi}{2} \le \varphi_n \le \frac{3\pi}{2} \end{cases}, \quad n = 1, 2, \ldots, N \tag{8}$$

where $\{\varphi_n\}_{n=1}^N$ are the azimuth angles of receivers in a counterclockwise direction, as shown in Figure 2. Although these angles are RVs, they are dependent on each other on the basis of the separation angles $\{\theta_n\}_{n=1}^N$. For any given receiver n, the azimuth angle is given by

$$\varphi_n = \varphi_q + \sum_{i=n}^{q-1}\theta_i, \quad n = 1, 2, \ldots, N \tag{9}$$

where q is a given aperture with angle φ_q. Note that $\{\theta_n\}_{n=1}^N$ are deterministic and fixed; therefore,

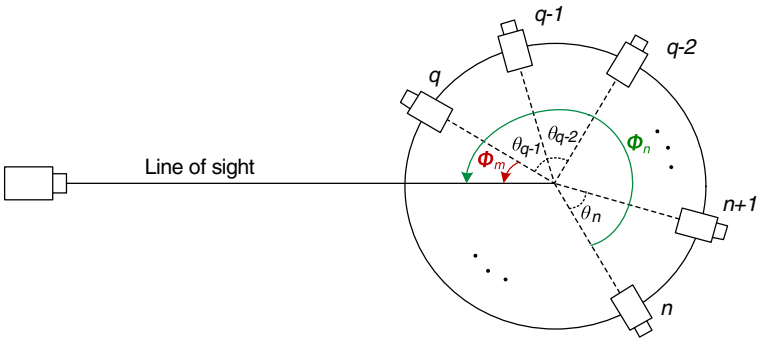

Figure 2. Angle analysis of nodes in a single-input multiple-output setup.

Equation (9) indicates that all RVs $\Phi = \{\varphi_n\}_{n=1}^{N}$ can be expressed in a single angle.

A small amount of symmetry can be included in the mobile node structure to characterize the received signal power within the branches. If the nodes are assumed to have uniform placement on the framework, then $\theta_1 = \theta_2 = \cdots = \theta_N = \theta$, which would be given by $\theta = 2\pi/N$. We can assume $q = 1$; thus,

$$\varphi_n = \varphi_1 + \frac{2(n-1)\pi}{N}, \quad n = 1, 2, \ldots, N \tag{10}$$

Equation (10) indicates that all RVs $\{\varphi_n\}_{n=1}^{N}$ are known if one of the variables is known. Thus, the RVs resulting from misalignment are entirely correlated and can be reduced to only one variable. If an RV, defined as $\varphi \triangleq \varphi_1$, and $-\pi/2 < \varphi < 3\pi/2$, has a PDF expressed by $f_\varphi(\varphi)$, then the PDF of all RVs are expressed by

$$f_{\varphi_n}(\varphi_n) = f_\varphi\left(\varphi - \frac{2(n-1)\pi}{N}\right), \quad n = 1, 2, \ldots, N \tag{11}$$

where $-\pi/2 < \varphi < 3\pi/2$. We assume variable φ has a uniform distribution as

$$f_\varphi(\varphi) = \frac{1}{2\pi}, \quad -\frac{\pi}{2} < \varphi < \frac{3\pi}{2} \tag{12}$$

Consequently, the PDF of α_n can be calculated from Equations (8) and (12) by

$$f_{\alpha_n}(\alpha_n) = \begin{cases} \delta(\alpha_n)\left(1 - \dfrac{1}{\pi}\displaystyle\int_{-\frac{\pi}{2}}^{\frac{\pi}{2}} \frac{\exp(\phi^2)}{2|\phi|}\mathrm{d}\phi\right) & \alpha_n = 0 \\ \dfrac{1}{2\pi\sqrt{\ln(1/\alpha_n)\alpha_n}} & 0 < \alpha_n \leq 1 \\ 0, & \alpha_n < 0 \text{ or } \alpha_n > 1 \end{cases} \tag{13}$$

where $n = 1, 2, \ldots, N$ and $0 \leq \alpha_n \leq 1$. Also, $f_{\alpha_n^2}(\alpha)$ is considered as the PDF of α_n^2, which becomes

$$f_{\alpha_n^2}(\alpha_n) = \frac{1}{2\alpha_n} f_{\alpha_n}(\alpha_n) \tag{14}$$

3.2. Transmitter misalignment

The implementation of a SIMO-based FSO system requires the divergence angle of the optical beam to be wide relative to receiver head size. In such a scenario, however, a very small sway of the transmitter will not cause a significant power fluctuation at the receiver side. The transmitter attenuation resulting from transmitter misalignment can be characterized in the analysis.

Farid and Hranilovic [11,12] have provided an analytical model that derives misalignment attenuation due to transmitter pointing error, given that a Gaussian beam is transmitted. The authors have investigated the resultant misalignment attenuation coefficient under circular aperture form, given by [11]

$$\beta_n \approx \exp\left(-\frac{2r_n^2}{\omega_{z_{\text{eq}}}^2}\right) \tag{15}$$

where r_n is the angular displacement for branch n and $\omega_{z_{\text{eq}}}$ is the parameter dependent on the beam propagation properties and aperture size. Specifically, $\omega_{z_{\text{eq}}}$ is the equivalent beam radius at the receiver. Additional details are available in [11]. In fact, $\omega_{z_{\text{eq}}}/2$ is the distance from the beam center where light intensity drops by a factor of e^{-2}. Assume that the SIMO transmitter has a misalignment pointing angle δ with respect to mobile FSO baseline, as shown in Figures 3 and 4. Such a radial pointing error is the result of both azimuth and elevation fluctuations of the transmitter. Arnon [13] has presented that fluctuations can be considered on the basis of an independent Gaussian distribution for elevation and horizontal directions. Thus, the amount of the radial pointing error has two degrees of freedom (DoF) with a Rayleigh distribution:

$$f_\delta(\delta) = \frac{\delta}{\sigma_\delta^2} \exp\left(-\frac{\delta^2}{2\sigma_\delta^2}\right) \tag{16}$$

where σ_δ is the overall pointing standard deviation. On the basis of symmetry, we assume that $\sigma_\delta = \sigma_v = \sigma_h$, where σ_v and σ_h are the elevation and azimuth pointing standard deviations, respectively. We can assume pointing

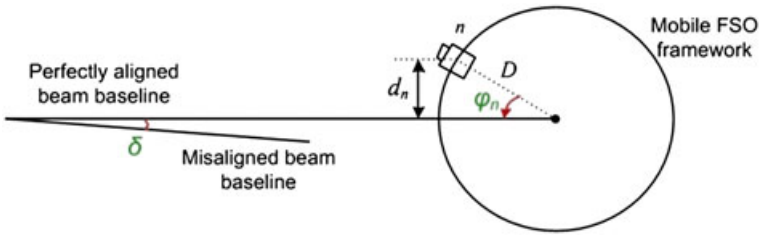

Figure 3. Radial displacement error due to transmitter misalignment. FSO, free space optics.

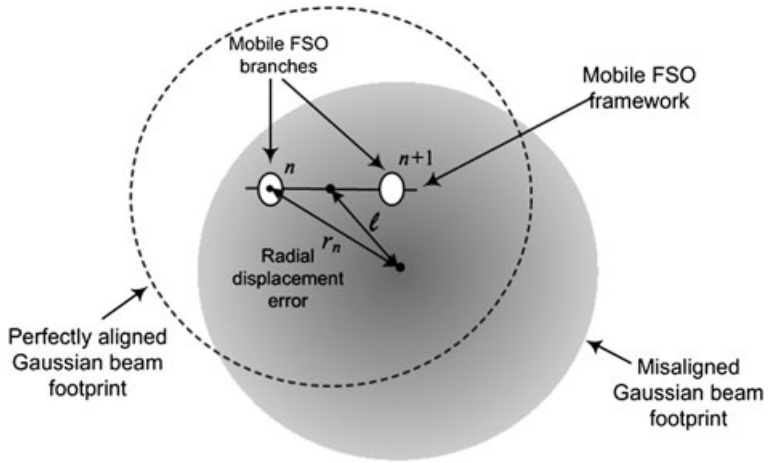

Figure 4. Radial displacement error due to transmitter misalignment. FSO, free space optics.

standard deviation, σ_δ, has a small value. Thus, the probability that $|\delta| \geq \pi/2$ is extremely insignificant. Assuming a significant propagation length relative to the diameter of the node's framework, that is, $L \gg D$, the displacement error at the receiver location, shown in Figure 3, is equal to $\ell = L\delta$, with a PDF of

$$f_\ell(\ell) = \frac{\ell}{\sigma_\delta^2} \exp\left(-\frac{\ell^2}{2L^2\sigma_\delta^2}\right), \ \ell \geq 0 \tag{17}$$

Given that the mobile FSO with radius D is small in comparison with the beam displacement, the overall displacement distance of a given branch n to the beam footprint center will be

$$r_n \approx \ell + d_n \tag{18}$$

where $d_n, d_n \leq D$, is the effective distance of the branch n to the beam center with no pointing error—either negative, zero, or positive. In accordance with Figure 3, d_n is given by

$$d_n = \sin(\varphi) D \tag{19}$$

which has a PDF of

$$f_{d_n}(d_n) = \frac{f_{\varphi_n}\left(\arcsin\left(\frac{d_n}{D}\right)\right)}{\sqrt{1-\left(\frac{d_n}{D}\right)^2}} \tag{20}$$

for $n = 1, 2, \ldots, N$. The marginal PDF of r_n is achieved through the convolution of the two PDFs, which leads to

$$f_{r_n}(r_n) = \int_{d_n} f_{d_n}(x) f_\ell(r_n - x) \mathrm{d}x \tag{21}$$

Assuming a uniform distribution for φ_1 in [0 to 2π], d_n varies from 0 to D; thus, the limit of integration in Equation (21) is available for

$$f_{r_n}(r_n) = \frac{1}{2\pi\sigma_\theta^2} \int_0^D \frac{r_n - x}{\sqrt{1-\left(\frac{x}{D}\right)^2}} \exp\left(-\frac{(r_n - x)^2}{2L^2\sigma_\theta^2}\right) \mathrm{d}x \tag{22}$$

which is identical for all branches $n = 1, 2, \ldots, N$. The marginal PDF of attenuation coefficient β_n can be computed by

$$f_{\beta_n}(\beta_n) = \frac{\omega_{z_{\mathrm{eq}}}^2}{4r_n'\beta_n} \left(f_{r_n}(r_n') + f_{r_n}(-r_n')\right) \tag{23}$$

where $r'_n \triangleq \omega_{z_{eq}}\sqrt{\ln(1/\sqrt{\beta_n})}$. Thus, $f_{\beta_n^2}(\beta_n)$ will be achievable by

$$f_{\beta_n^2}(\alpha_n) = \frac{1}{2\beta_n} f_{\beta_n}(\beta_n) \tag{24}$$

3.3. The correlation

The instantaneous received SNR of a specified branch n is given by Equation (2) with a PDF described by Equation (7). As previously mentioned, turbulence coefficients are uncorrelated. Thus, all RVs h_n, α_n, and β_n and consequently h_n^2, α_n^2, and β_n^2 are uncorrelated, as they are produced from different independent sources. The correlation between SNRs for various branches is established in the following.

Let us assume two different receiving illuminated branches i and j on the framework, that is, $-\pi/2 < \varphi_i, \varphi_j < \pi/2$. The covariance function for both variables γ_i and γ_j is calculated by

$$q_{i,j} = E[\gamma_i \gamma_j] - E[\gamma_i]E[\gamma_j] \tag{25}$$

The conditional covariance function, $\hat{q}_{i,j}$, must first be calculated given misalignment states $\alpha_i, \alpha_j, \beta_i$, and β_j, and then

$$q_{i,j} = E[\hat{q}_{i,j}] \tag{26}$$

is applied. With γ_i and γ_j being replaced from Equation (2), the covariance will be

$$\begin{aligned}\bar{q}_{i,j} &= \bar{\gamma} E\left[h_i^2 h_j^2 \alpha_i^2 \alpha_j^2 \beta_i^2 \beta_j^2 \middle| \alpha_i, \alpha_j, \beta_i, \beta_j\right] \\ &\quad - \bar{\gamma} E\left[h_i^2 \alpha_i^2 \beta_i^2 \middle| \alpha_i, \beta_i\right] E\left[h_j^2 \alpha_j^2 \beta_j^2 \middle| \alpha_j, \beta_j\right] \\ &= \bar{\gamma} E\left[h_i^2\right] E\left[h_j^2\right] \alpha_i^2 \alpha_j^2 \beta_i^2 \beta_j^2 \\ &\quad - \bar{\gamma} E\left[h_i^2\right] E\left[h_j^2\right] \alpha_i^2 \alpha_j^2 \beta_i^2 \beta_j^2 \\ &= 0\end{aligned} \tag{27}$$

Equation (27) indicates that the covariance between branch SNRs in Equation (25) is zero; thus, the branches have uncorrelated SNR values.

In the analysis previously, it is assumed that the paths are associated with illuminated branches. The SNR of non-illuminated branches, however, is zero. Assuming an even number of branches for the circular configuration provided, we can conclude that only $N/2$ of those are illuminated by the beam. In fact, the number of effective branches is actually cut in half. Thus, the representation of node SNRs is presented for $n = 1, \ldots, N/2$ by

$$\begin{aligned}f_{\gamma_n}(\gamma_n) = &\frac{1}{\bar{\gamma}} \int_0^1 \frac{1}{\beta_n^2} f_{\beta_n^2}\left(\frac{\gamma_n}{\beta_n^2}\right) \int_0^1 \frac{1}{\alpha_n^2} f_{h^2}(\alpha_n) f_{\alpha_n^2} \\ &\times \left(\frac{\beta_n^2}{\bar{\gamma}\alpha_n^2}\right) \mathrm{d}\alpha_n \mathrm{d}\beta_n\end{aligned} \tag{28}$$

as given by Equation (7); the SNR is zero for non-illuminated branches:

$$f_{\gamma_n}(\gamma_n) = 0, \quad n = \frac{N}{2} + 1, \ldots, N \tag{29}$$

4. THE SWITCH-AND-EXAMINE COMBINING APPROACH

Signals from receiver apertures require combining prior to detection, as shown in Figure 5. In this section, the authors statistically depict SEC-switched diversity for mobile FSO.

Unlike SC diversity, switched diversity does not require persistent monitoring of all receiving signals. Instead, the scheme eliminates unnecessary monitoring and repetitive switching, resulting in a lower processing load at the combiner. This outcome proves significant, especially given that FSO applications are subject to a high processing load as a consequence of high data rate communication.

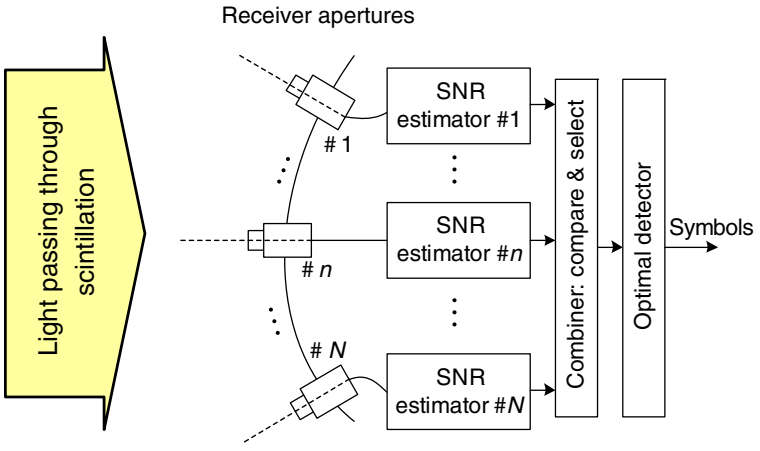

Figure 5. Structure of an unbalanced multireceiver. SNR, signal-to-noise ratio.

4.1. Switching strategy

Only a handful of diversity approaches are potentially viable for switched diversity. Based on a switch-and-stay combining (SSC) scheme [14,15], the combiner switches to a new branch only after the existing received SNR falls below a threshold γ_T. This switching occurs regardless of the new branch SNR—even if it is inferior to the original branch. A major deficiency for SSC is the high probability that the optical beam will fail to illuminate the receiving branch, that is, half of the receivers are not illuminated, rendering it an unacceptable choice for mobile FSO.

The SEC diversity scheme is similar to SSC, albeit with minor modification. A low SNR reading initiates branch switching; however, the SNR of the new branch is considered first, for example, if the SNR is above the threshold level, the original branch is maintained. Branch evaluation continues to alternate branches until an acceptable SNR is observed, and a branch selection is made. SEC is designed on a switching threshold basis and proposes to reduce the volume of processing load and thus implementation complexity in the receiver design [14,16].

The SEC approach has been characterized by Yang and Alouini in [17] and Alexandropoulos *et al.* in [16] Simon and Alouini [14, Equation (9.340)] have rewritten the result from these two uncorrelated paths. This paper proposes a similar but more basic method for characterizing the probability distribution of the resultant SNR for FSO links, as shown later.

4.2. Analytical analysis

Let us include the discrete time index k in the analytical discussion. For a receiver with N branches (N even), only $M \triangleq N/2$ branches illuminated by the incident beam participate in the combining process. Without loss of generality, suppose the combiner is currently connected to branch n of an N-branch receiver. To avoid confusion, we recall several notation definitions as follows:

$\gamma_n[k]$:	instantaneous received SNR at branch n at time k
$\gamma[k]$:	combined (resultant) received SNR at time k
γ:	combined (resultant) received SNR variable
n:	active branch at time k
γ_T:	switching threshold

We emphasize that γ_n is the total instantaneous SNR at receiver n; thus, the analysis is applicable to SIMO configuration. Because sequence events $\{\gamma[k] = \gamma_i[k]\}_{i=1}^{M}$ are mutually exclusive, the cumulative distribution function (CDF) of the resultant SNR can be generally rewritten as [17,18]

$$F_{\mathrm{SEC}}(\gamma) = \sum_{i=1}^{M} P(\gamma[k] = \gamma_i[k] \text{ and } \gamma_i[k] \le \gamma) \quad (30)$$

By considering the mutually exclusive property of sequence $\{\gamma[k] = \gamma_i[k]\}_{i=1}^{M}$, the CDF can be deduced from Equation (30):

$$F_{\mathrm{SEC}}(\gamma) = MP(\gamma[k] = \gamma_n[k] \text{ and } \gamma_n[k] \le \gamma) \quad (31)$$

Given SEC switching strategy, there are a number of possible cases in which equality $\gamma[k] = \gamma_n[k]$ may occur, where

$$\gamma[k] = \gamma_n[k] \text{ iff } \begin{cases} \gamma[k-1] = \gamma_{n-1}[k-1] \\ \text{and } \gamma_{n-1} < \gamma_T \text{ and } \gamma_n[k] \ge \gamma_T \\ \quad \text{or} \\ \gamma[k-1] = \gamma_{n-2}[k-1] \\ \text{and } \bigcap_{1=n-2}^{n-1} \gamma_i[k] < \gamma_T \text{ and } \gamma_n[k] \ge \gamma_T \\ \quad \text{or} \\ \quad \vdots \\ \gamma[k-1] = \gamma_1[k-1] \\ \text{and } \bigcap_{i=1}^{n-1} \gamma_i[k] < \gamma_T \text{ and } \gamma_n[k] \ge \gamma_T \\ \quad \text{or} \\ \gamma[k-1] = \gamma_M[k-1] \\ \text{and } \bigcap_{i=N}^{n-1} \gamma_i[k] < \gamma_T \text{ and } \gamma_n[k] \ge \gamma_T \\ \quad \text{or} \\ \quad \vdots \\ \gamma[k-1] = \gamma_{n+1}[k-1] \\ \text{and } \bigcap_{i=n+1}^{n-1} \gamma_i[k] < \gamma_T \text{ and } \gamma_n[k] \ge \gamma_T \\ \quad \text{or} \\ \gamma[k-1] = \gamma_n[k-1] \text{ and } \gamma_n[k] \ge \gamma_T \end{cases} \quad (32)$$

Equation (23) lists all possible cases in which the nth receiver is the current receiver at time k. Because receiver apertures are symmetrically placed on the platform, $\cap_{i=t}^{s} \gamma_i[k] < \gamma_T$ for $t > s$ becomes

$$\bigcap_{i=t}^{s} \gamma_i[k] \triangleq \left(\bigcap_{i=t}^{M} \gamma_i[k] \right) \bigcap \left(\bigcap_{i=1}^{s} \gamma_i[k] \right) \quad (33)$$

recalling that events $\gamma[k-1] = \gamma_i[k-1], i = 1, 2, \ldots, M$, are mutually exclusive. Consequently, any "and" combination will also be exclusive. Branches are equally likely to be selected because of the symmetry of receiver apertures on the platform. Thus, applying the occurrence probability of each case (exclusive of the last term) as $1/(M-1)$ in

Equation (32) and by substituting the simplified expression in the CDF in Equation (30) yields

$$F_{\mathrm{SEC}}(\gamma) = \frac{M}{M-1}\sum_{j=1}^{M} P\left\{\begin{array}{l}\gamma[k-1]=\gamma_q[k-1] \text{ and } \gamma_n[k]\geq\gamma_{\mathrm{T}} \\ \text{and } \bigcap_{i=n-1-j}^{n-1}\gamma[k]=\gamma_{\mathrm{T}} \text{ and } \gamma_n[k]\geq\gamma\end{array}\right\} + MP\left\{\begin{array}{l}\gamma[k-1]=\gamma_n[k-1] \text{ and } \gamma_n[k]\geq\gamma_{\mathrm{T}} \\ \text{and } \gamma_n[k]\leq\gamma\end{array}\right\} \tag{34}$$

The combiner monitors instantaneous SNR at a combining iteration period that is amply large when compared with coherence time. Consequently, the uncorrelated pair $\gamma_n[k]$ and $\gamma_q[k]$ are independent of their corresponding values at time $k-1$. By understanding that $P\{\gamma[k] = \gamma_n[k]\} = 1/M$ and, similarly, $P\{\gamma[k-1] = \gamma_n[k-1]\} = 1/M$ for any value of n, CDF is evaluated in the form

$$F_{\mathrm{SEC}}(\gamma) = \frac{1}{M-1}\sum_{j=1}^{M-1} P\left\{\bigcap_{i=n-j}^{n-1}\gamma_i[k]=\gamma_{\mathrm{T}}\cap\gamma_{\mathrm{T}}\leq\gamma_n[k]\leq\gamma\right\} + P\{\gamma_n[k]\geq\gamma_{\mathrm{T}} \text{ and } \gamma_n[k]\leq\gamma\} \tag{35}$$

Depending on the value of γ_{T}, $F_{\mathrm{SEC}}(\gamma)$ converts to

$$F_{\mathrm{SEC}}(\gamma) = \begin{cases} G_\gamma(\gamma) & \gamma<\gamma_{\mathrm{T}} \\ F_\gamma(\gamma)-F_\gamma(\gamma_{\mathrm{T}})+G_\gamma & \gamma\geq\gamma_{\mathrm{T}}\end{cases} \tag{36}$$

where $F_\gamma(\cdot)$ is the marginal CDF of the resultant SNR, γ. Recalling that n can be any given branch $n \in \{1, 2, \ldots, M\}$, simply by choosing $n = M$, $G_\gamma(\gamma)$ is calculated by

$$G_\gamma(\gamma) = \frac{M}{M-1}\sum_{j=1}^{M-1} P\left\{\bigcap_{i=n/2-j}^{n-1}\gamma_i[k]\leq\gamma_{\mathrm{T}} \text{ and } \gamma_M[k]\leq\gamma\right\} \tag{37}$$

which extends to

$$\begin{aligned} G_\gamma(\gamma) = \frac{M}{M-1}\{&P\{\gamma_{m-1}[k]\leq\gamma_{\mathrm{T}} \text{ and } \gamma_M[k]\leq\gamma\} \\ &+ P\{\gamma_{M-2}[k]\leq\gamma_{\mathrm{T}} \text{ and } \gamma_{M-1}[k]\leq\gamma_{\mathrm{T}} \\ &\quad \text{and } \gamma_M[k]\leq\gamma\}+\cdots \\ &+ P\{\gamma_1[k]\leq\gamma_{\mathrm{T}}\ldots \text{ and } \gamma_{M-1}[k]\leq\gamma_{\mathrm{T}} \\ &\quad \text{and } \gamma_M[k]\leq\gamma\}\}\end{aligned} \tag{38}$$

To provide a clear understanding of Equation (38), we illustrate that for an M-branch combiner

$$\begin{aligned} &P\{\gamma_1[k]\leq\gamma_{\mathrm{T}}\ldots \text{ and } \gamma_{K-1}[k]\leq\gamma_{\mathrm{T}} \text{ and } \gamma_K[k]\leq\gamma\} \\ &= \underbrace{\int_0^{\gamma_{\mathrm{T}}}\cdots\int_0^{\gamma_{\mathrm{T}}}}_{K-1}\left(f_{\gamma_n}(\gamma_n)\right)^{K-1}\mathrm{d}\gamma_n \\ &\quad\times\underbrace{\int_0^{\infty}\cdots\int_0^{\infty}}_{M-K}\left(f_{\gamma_n}(\gamma_n)\right)^{M-K}\mathrm{d}\gamma_n \\ &\quad\times\int_0^{\gamma} f_{\gamma_n}(\gamma_n)\mathrm{d}\gamma_n\end{aligned} \tag{39}$$

for any integer $2 \leq K \leq M$. The PDF of the resultant γ can be mathematically expressed by

$$f_{\mathrm{SEC}}(\gamma) = \begin{cases} g_\gamma(\gamma) & \gamma<\gamma_{\mathrm{T}} \\ f_\gamma(\gamma)+g_\gamma(\gamma) & \gamma\geq\gamma_{\mathrm{T}}\end{cases} \tag{40}$$

where $f_\gamma(\gamma)$ is the marginal PDF derivable from Equation (7) and $g_\gamma(\gamma) \triangleq (\mathrm{d}/\mathrm{d}_\gamma)G_\gamma(\gamma)$. By applying an optimal detection for an extremely large number of symbols, the average BER is achievable by

$$P^e_{\mathrm{SEC}} = \int_0^{\infty} f_{\mathrm{SEC}}(\gamma)Q(\sqrt{\gamma})\mathrm{d}\gamma \tag{41}$$

where $Q(\cdot)$ is one-dimensional Q-function.

5. SIMULATION ANALYSIS

This section provides numerical evaluation of mobile FSO over average atmospheric turbulence and node mobility. BER is numerically measured by sending intensity-modulated symbols through a fading channel and then detecting the received symbols using an optimal detector. We assume the mobile FSO has N receiving apertures installed unbalanced on a framework of $D = 20$ cm with a transmission length of $L = 1$ km. Additional processing load (APL) due to diversity is defined as the number of monitoring occurrences of inactive branches to the total number of branches. Subsequently, the processing load for SC is $N-1$ and for SEC is $\epsilon\xi/\tau$, where ϵ is the number of inactive branch monitoring occurrences in a period τ and ξ is the combining iteration period. Based on SEC switching strategy, $APL \leq N-1$, indicating that it is always less than SC.

A symbol-by-symbol detection method is used, assuming perfect CSI in Equation (4) is available. On–off keying modulation is employed for simulation purposes. When referred, definition $\bar{\gamma}$ in Equation (3) is used as the *average branch SNR* in the performance plots. To normalize the power, we include $2RP_t = 1$. Lognormal distribution is applied for channel fading distribution with independent samples. By default, fading turbulence is considered to be average by setting $\gamma_\chi = 0.1$. We assume uniform but independent distributions for misalignment angle φ_1 through PDFs $f_\varphi(\varphi)$, changing from $-\pi/2$ and $3\pi/2$. By using

Equation (10), all other variables $\{\varphi_n\}_{n=2}^{N}$ can be determined. Any misalignment gain factor of $\{\alpha_n\}_{n=1}^{N}$ has a value between 0 and 1, given in Equation (8). For transmitter misalignment, we include $\omega_{z\,\mathrm{eq}} = 3$ m with a fluctuation standard deviation in the range of $\gamma_\varphi = 2 \times 10^{-4}$ to calculate the misalignment statistics of $\{\beta_n\}_{n=1}^{N}$ in Equation (15). Under this value for γ_φ, the corresponding jitter standard deviation will be equal to $L\gamma_\varphi = 20$ cm.

It is possible that an optimum threshold for SEC that minimizes BER performance may indeed exist, as shown in Figure 6. For high values of γ_T, the combiner is unable to find an acceptable branch, thus remains locked to one branch. Hence, SEC works as an unbalanced single receiver. For low values of γ_T, the situation is far superior as the chance of switching is higher than when large γ_T values are chosen. Optimal points will be applied in forthcoming simulations.

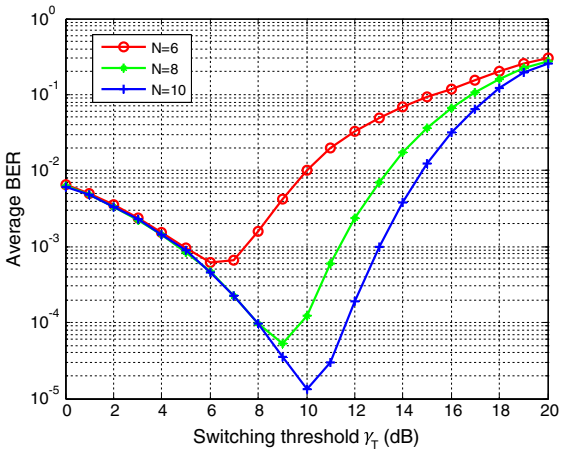

Figure 6. Bit error rate (BER) versus switching threshold γ_T, for an *N*-branch mobile free space optics with switch-and-examine combining. $\sigma_\chi = 0.1$, $\sigma_\delta = 2x10^{-3}$, and $\bar{\gamma} = 20$ dB.

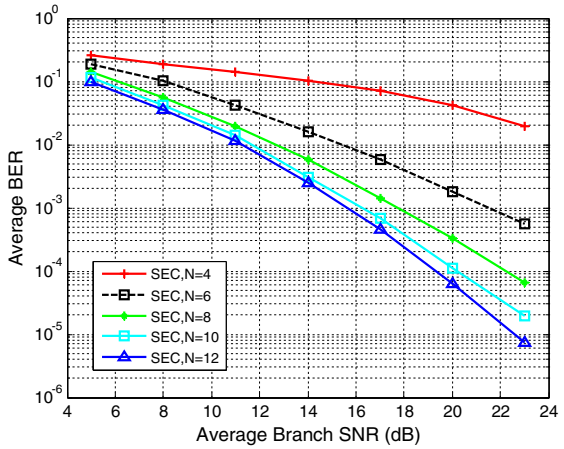

Figure 7. Optimal performance of switch-and-examine combining (SEC) for mobile free space optics versus $\bar{\gamma}$, for $N = 4 - 12$ at $\sigma_\chi = 0.1$ and $\sigma_\delta = 2 \times 10^{-3}$. BER, bit error rate.

Figure 7 is presented to highlight the effect of the number of branches on SEC BER performance. As demonstrated, $N = 4$ results in poor mobile FSO performance. Compared with the performance at $N = 6$, the BER performance loss at an SNR equal to $\bar{\gamma} = 20$ dB is about 10 dB. However, this loss is negligible, for example, 1 dB, when the number of branches is decreased from $N = 12$ to $N = 10$. Figure 8 compares SC and SEC BER performances. SC performance is superior, for example, the BER performance of SC having $N = 6$ is superior to that of SEC with $N = 8$, which is approximately 2.2 dB at $\bar{\gamma} = 20$ dB. Figure 9 exhibits the effect of σ_δ on BER performance.

Processing load resulting from a combining performance criterion is presented in Table I . When compared with SC performance, SEC decreases the processing load in the combiner. The amount of saving is listed in Table I

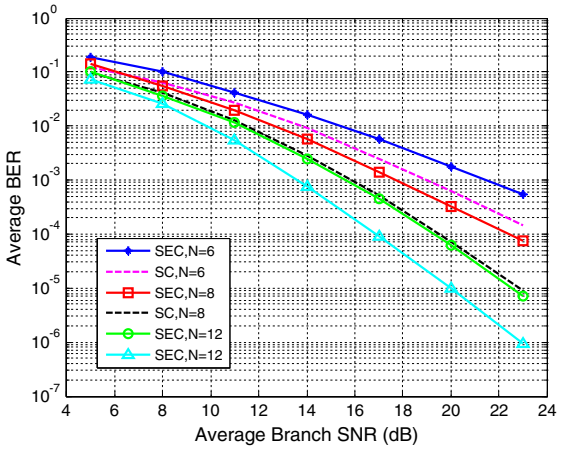

Figure 8. Performance of switch-and-examine combining (SEC) for mobile free space optics compared with selection combining (SC) for $N = 6, 8, 12$ at $\sigma_\chi = 0.1$ and $\sigma_\delta = 2 \times 10^{-3}$.

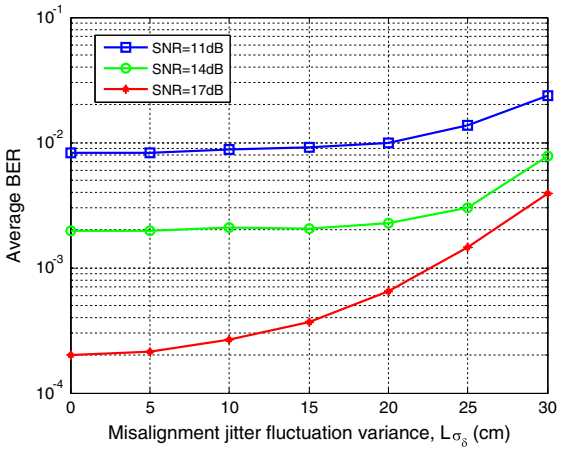

Figure 9. The effect of pointing standard deviation on the bit error rate (BER) performance of switch-and-examine for mobile free space optics. $N = 4$, $\sigma_\chi = 0.2$, and $\bar{\gamma} = 17$ dB. SNR, signal-to-noise ratio.

Table I. Saving in combiner's processing load for switch-and examine combining relative to selection combining at $\gamma_\chi = 0.1$ and $\gamma_\delta = 2 \times 10^{-3}$.

Signal-to-noise ratio (dB)	Saving in processing load (%)		
	$N = 6$	$N = 8$	$N = 12$
$\bar{\gamma} = 5$	47.95	51.39	55.85
$\bar{\gamma} = 14$	63.70	64.09	64.16
$\bar{\gamma} = 23$	65.70	65.45	65.50

for $N = 6, 8, 12$. Increasing the number of branches contributes to a higher load for both SC and SEC. For low SNR values, for example, $\bar{\gamma} = 5$ dB, the saving for SEC compared with that for SC is nearly unchanged.

6. CONCLUSIONS

Deployment of mobility-based FSO links is complicated because highly sensitive FSO links are subject to misalignment. This paper proposes and then analyzes a circular structure for mobile FSO apertures by providing mobility to FSO nodes in wireless sensor networks and mobile ad hoc networks. In this work, mobile FSO was evaluated under SIMO configuration. A small number of receiver apertures were intentionally misaligned to provide angular diversity. The transmitted laser beam is assumed as Gaussian profile undergone by transmitter sway fluctuations. Channels are considered uncorrelated under average turbulence conditions. Accordingly, an SEC diversity technique is suggested for combining purposes because of its low processing load; however, an optimal switching threshold is required for performance optimization.

ACKNOWLEDGEMENTS

The computing for this project was performed at the OU Supercomputing Center for Education & Research (OSCER) at the University of Oklahoma (OU).

This work is funded by NSF grant number NSF-ECCS 1002288 and was presented in part at the IWCMC '11 conference, Istanbul, Turkey, in July 2011.

REFERENCES

1. Yan P, Sluss Jr JJ, Refai HH, LoPresti PG. Enhancing mobile ad hoc networks with free-space optics. *SPIE Journal of Optical Engineering* 2007; **46**: 1–7.
2. Ghosh AK, Kunta S, Verma P, Huck RC. Free-space optics based sensor network design using angle-diversity photodiode arrays. *Proceedings of the SPIE* 2010; **7814**: 1–7.
3. Cap GA, Refai HH, Sluss Jr JJ. FSO tracking and auto-alignment transceiver system. *Proceedings of the SPIE* 2008; **7112**: 1–12.
4. Nakhkoob B, Bilgi M, Yuksel M, Hella M. Multi-transceiver optical wireless spherical structures for MANETs. *IEEE Journal on Selected Area in Communications* 2009; **27**(9): 1612–1622.
5. Yuksel M, Akella J, Kalyanaraman S, Dutta P. Free-space-optical mobile ad hoc networks: auto-configurable building blocks. *ACM/Springer Wireless Networks* 2009; **15**(3): 295–312.
6. Alattar JM, Elmirghani JMH. Optical wireless systems employing adaptive collaborative transmitters in an indoor channel. *IEEE Transactions on Vehicular Technology* 2010; **59**(1).
7. Moradi H, Refai HH, LoPresti PG. Thresholding-based optimal detection of wireless optical signals. *IEEE/OSA Journal of Optical Communications and Networking* 2010; **2**(9): 689–700.
8. Zhu X, Kahn JM. Free-space optical communication through atmospheric turbulence channels. *IEEE Transactions on Communications* 2002; **50**(8): 1293–1300.
9. Osche GR. *Optical Detection Theory for Laser Applications*. John Wiley & Sons, Inc: Hoboken, NJ, 2002.
10. Gray JE, Addison SR. Characteristic functions in radar and sonar, In *Proceedings of the 34th Southeastern Symposium on System Theory*, Huntsville, Alabama, 2002; 31–35.
11. Farid AA, Hranilovic S. Outage capacity optimization for free-space optical links with pointing errors. *Journal of Lightwave Technology* 2007; **25**(7): 1702–1710.
12. Farid AA, Hranilovic S. Diversity gains for MIMO wireless optical intensity channels with atmospheric fading and misalignment, In *IEEE Globecom '10 Workshops*, 2010; 1015–1019.
13. Arnon S. Effects of atmospheric turbulence and building sway on optical wireless-communication systems. *Optics Express* 2003; **28**(2): 129–131.
14. Simon MK, Alouini MS. *Digital Communication over Fading Channels*, 2nd ed. John Wiley & Sons, Inc: Hoboken, NJ, 2005.
15. Ko YC, Alouini MS, Simon MK. Analysis and optimization of switched diversity systems. *IEEE Transactions on Vehicular Technology* 2000; **49**(5): 1813–1831.
16. Alexandropoulos GC, Mathiopoulos PT, Sagias NC. Switch-and-examine diversity over arbitrarily correlated Nakagami-*m* fading channels. *IEEE Transactions on Vehicular Technology* 2010; **59**(4): 2080–2087.
17. Yang HC, Alouini M-S. Performance analysis of multibranch switched diversity systems. *IEEE Transactions on Communications* 2003; **51**(5): 782–794.
18. Abu-Dayya AA, Beaulieu NC. Analysis of switched diversity systems on generalized-fading channels. *IEEE Transactions on Communications* 1994; **42**(11): 2259–2966.

AUTHORS' BIOGRAPHIES

Hassan Moradi received his B.Sc. and Master's degrees in Electrical Engineering-Communications from Shiraz University, Shiraz, Iran, and K.N. Toosi University of Technology, Tehran, Iran, in 1998 and 2001, respectively. Prior to joining the University of Oklahoma, he served from 2001 to 2007 as Senior Research Associate for Iran Telecom Research Center (ITRC). Currently, Hassan is a Ph.D. candidate in the Department of Electrical and Computer Engineering, University of Oklahoma-Tulsa. His primary research interest is MIMO and diversity for optical wireless communications. His field of interest also includes multiple access techniques in wireless networks and network signaling protocols.

Hazem H. Refai received his M.S.E.E. and Ph.D. degrees from the University of Oklahoma-Norman in 1993 and 1999, respectively. Currently, he is an associate professor at the School of Electrical and Computer Engineering (ECE) Telecommunication Program in Tulsa, OK. He is the founder and director of the Wireless Electromagnetic Compliance and Design (WECAD) Center. The Center's mission is to carry out basic and applied research in RF and optical wireless communication and networks as well as electromagnetic compatibility. His fields of interest include the development of physical and medium access control layers for mobile laser communication networks using free space optics, cognitive radios and networks, sensor-based auto-collision avoidance system, vehicle-to-vehicle communication protocols, and portable hybrid RF/FSO communication systems for disaster recovery.

Peter G. LoPresti received his B.S.E. degree in Electrical Engineering from the University of Delaware, Newark, in 1988, and his Ph.D. degree in Electrical Engineering from The Pennsylvania State University, University Park, in 1994. Currently, he is a professor of Electrical Engineering at The University of Tulsa, Tulsa, OK. He currently acts as a consultant on the development of three-dimensional displays and is the Director of the Williams Communications Optical Networking Laboratory at the University of Tulsa. His fields of interest include the engineering of optical communications systems; the design and implementation of mobile free-space optical communication networks for disaster recovery, environmental monitoring, and battlefield communication; and optical sensor development for environmental monitoring.

Mohammeed Atiquzzaman obtained his M.S. and Ph.D. in Electrical Engineering and Electronics from the University of Manchester (UK). He currently holds the Edith Kinney Gaylord Presidential professorship in the School of Computer Science at the University of Oklahoma and is a senior member of IEEE. Atiquzzaman is the editor-in-chief of Journal of Networks and Computer Applications and serves on the editorial boards of IEEE Communications Magazine, International Journal on Wireless and Optical Communications, Real Time Imaging journal, Journal of Communication Systems, Communication Networks and Distributed Systems, and Journal of Sensor Networks. He has served as co-chair of IEEE High Performance Switching and Routing Symposium and has served as symposium co-chairs for IEEE Globecom and IEEE ICC conferences. He is the co-author of the book "Performance of TCP/IP over ATM Networks" and has over 250 refereed publications.

Wirel. Commun. Mob. Comput. 2011; **11**:1540–1550 © 2011 John Wiley & Sons, Ltd.
DOI: 10.1002/wcm